Appl. Phys. A (2015) 120:1615–1623
DOI 10.1007/s00339-015-9371-1

Applied Physics A
Materials Science & Processing

Synthesis, photoluminescence and Judd–Ofelt parameters of $LiNa_3P_2O_7:Eu^{3+}$ orthorhombic microstructures

K. Munirathnam[1,8] · G. R. Dillip[2] · B. Deva Prasad Raju[1,3] · S. W. Joo[2] · S. J. Dhoble[4] · B. M. Nagabhushana[5] · R. Hari Krishna[5] · K. P. Ramesh[6] · S. Varadharaj Perumal[7] · D. Prakashbabu[8]

Received: 24 June 2015 / Accepted: 14 July 2015 / Published online: 25 July 2015

Abstract We report, for the first time, the photoluminescence properties of Eu^{3+}-doped $LiNa_3P_2O_7$ phosphor, synthesized by a facile solid-state reaction method in air atmosphere. The crystal structure and phase purity of the phosphors were analyzed by X-ray diffraction analysis. Orthorhombic structural morphology was identified by scanning electron microscopy. The phosphate groups in the phosphor were confirmed by Fourier transform infrared analysis. Bandgap of the phosphor was calculated from the diffuse reflectance spectra data using Kubelka–Munk function. Under 395-nm UV excitation, the phosphors show signs of emitting red color due to the $^5D_0 \rightarrow {}^7F_2$ transition. In accordance with Judd–Ofelt theory, spectroscopic parameters such as oscillator intensity parameter Ω_t ($t = 2$), spontaneous emission probabilities, fluorescence branching ratios and radiative lifetimes were calculated and analyzed for the first time in this system.

✉ G. R. Dillip
dillip.ngr@gmail.com

✉ B. Deva Prasad Raju
drdevaprasadraju@gmail.com

✉ S. W. Joo
swjoo@yu.ac.kr

[1] Department of Physics, Sri Venkateswara University, Tirupati 517 502, India

[2] School of Mechanical Engineering and Technology, Yeungnam University, Gyeongsan 712-749, South Korea

[3] Department of Future Studies, Sri Venkateswara University, Tirupati 517 502, India

[4] Department of Physics, R.T.M. Nagpur University, Nagpur 440 033, India

[5] Department of Chemistry, M.S. Ramaiah Institute of Technology, Bangalore 560 054, India

[6] Department of Physics, Indian Institute of Sciences, Bangalore 560 012, India

[7] Centre for Nanosciences and Technology, Indian Institute of Sciences, Bangalore 560 012, India

[8] School of Physical Sciences, Reva University, Bangalore 560 064, India

1 Introduction

Nowadays, the preparation of rare-earth (RE) ions-activated inorganic phosphor materials has engrossed extensive attention due to their potential applications in fabricating primitive white light-emitting diodes (w-LEDs) and luminescent devices for new generation [1–3]. w-LEDs offer various benefits in terms of energy saving, high reliability, low maintenance cost and positive environment effects and are a competent of replacing the traditional light sources such as incandescent and fluorescent lamps [4]. One way of designing white LEDs is incorporating the red-, green- and blue-emitting phosphors on an UV LED [5, 6]. In order to develop practically applicable w-LEDs, novel tricolor phosphors are requisite which could be effectively excited by near-UV radiation. The efficient red-emitting phosphors are still limited for the enhancement of color rending index (CRI) of white LEDs [7, 8]. Hence, there has been a widespread and growing interest in the development of novel materials of red-emitting phosphors with high absorption in the near-UV radiation, excellent color rendering index, high color tolerance and high conversion efficiency into visible light.

Trivalent Eu^{3+} ions are expected to be one of the promising species in different host materials that undergo optical transitions and give out radiation in red color region. Over the past few decades, many researches have

been devoted to synthesizing the Eu-activated silicates ($(Ba,Ca,Sr)_3MgSi_2O_8$, Li_2SrSiO_4) [9, 10], aluminates ($CaAl_2O_4$, $ZnMgAl_{11}O_{17}$) [11, 12], borates ($NaSrBO_3$, $YAl_3(BO_3)_4$) [13, 14], phosphates ($CaMgP_2O_7$, $Na_2CaMg(PO_4)_2$) [15, 16], etc. Among them, the preparation of Eu^{3+}-doped orthophosphates was given more importance, since they are promising host materials because of their ease of synthesis, low cost and chemical and thermal stabilities over a wide range of temperature [17].

From the survey of the literature, it has been noticed that there are no results appeared on the photoluminescence studies of Eu^{3+}-activated pyrophosphate ($LiNa_3P_2O_7$). In addition, J–O theory has not been applied uniformly to characterize the spectroscopic properties of Eu^{3+} ion in polycrystalline powders of $LiNa_3P_2O_7$ (to our knowledge). In the present investigation, the synthesis of new host matrix, $LiNa_3P_2O_7$ doped with Eu^{3+} ions, has been reported to study their spectroscopic properties for the first time. Additionally, the J–O parameters were calculated to understand their radiative properties. Finally, the important parameters to be applied for w-LEDs such as color coordinates and color temperature were calculated and reported for this system.

2 Experimental

2.1 Synthesis

The pyrophosphate phosphors, $LiNa_{3-x}P_2O_7{:}xEu^{3+}$ ($x = 0$, 1, 3, 5, 7 and 9 at.%), were synthesized using a traditional solid-state reaction method. The high-purity (99.99 %) chemicals of Li_2CO_3, Na_2CO_3, $NH_4H_2PO_4$ and Eu_2O_3 (Sigma-Aldrich, USA) were used as starting materials without further purification. First, the stoichiometric amounts of starting materials were mixed together in an agate mortar. Since the materials are rich in ammonium (NH_3) and carbon dioxide (CO_2), the mixture was preheated at 400 °C for 3 h to release the excess of gases. Further, the obtained mixtures are reground and then calcined at 540 °C for 18 h with several intermediate grindings. The final products were obtained by cooling down to room temperature (RT) in the furnace, thereafter ground again into fine powder, and used for further characterization.

2.2 Characterization

The phase purity of prepared $LiNa_{3-x}P_2O_7{:}xEu^{3+}$ phosphors was analyzed by X-ray diffraction (XRD) using PANalytical diffractometer (Siemens, AXS D5005) with Cu–K_α radiation of wavelength 1.540 Å at a scanning step size of 0.02°. The data were collected in the range from 10° to 60° at 40 kV and 20 mA. Fourier transform infrared (FTIR) spectrum of phosphor was recorded by using a Bruker IFS Equinox 55 FTIR spectrometer in the range of 400 to 4000 cm^{-1}. The surface morphology of the powder phosphor was inspected using a scanning electron microscopy (ZEISS EVO MA 15). The elemental composition was quantified by energy-dispersive spectroscopy (EDS) using an X-ray detector (THERMO EDS) attached to the SEM instrument. UV–Vis diffuse reflectance spectra were recorded on V-670 UV–Vis–NIR spectrophotometer (JASCO, JAPAN). The excitation spectrum was recorded by monitoring emission at 613 nm, and emission spectra were obtained at an excitation wavelength of 395 nm using fluorescence spectrophotometer (Jobin Vyon Fluorolog-3). All the measurements were taken at RT.

3 Results and discussion

3.1 XRD analysis

In order to identify the crystal structure of the $LiNa_{3-x}P_2O_7{:}xEu^{3+}$ phosphor, the XRD analysis was carried out. The typical XRD pattern of undoped and 7 at.% doped $LiNa_{3-x}P_2O_7{:}xEu^{3+}$ phosphor is shown in Fig. 1. All the reflections observed in the phosphor were well matched with the reported crystal structure of $LiNa_3P_2O_7$ by Shi et.al. [18] and Zaafouri et al. [19]. According to them, the $LiNa_3P_2O_7$ has been reported to crystallize in the orthorhombic structure with the space group C_{2221} and the lattice parameters are $a = 5.4966$ Å, $b = 9.1365$ Å and $c = 12.2764$ Å. In comparison with the undoped sample, 7 at.% Eu-doped phosphor exhibits similar reflections

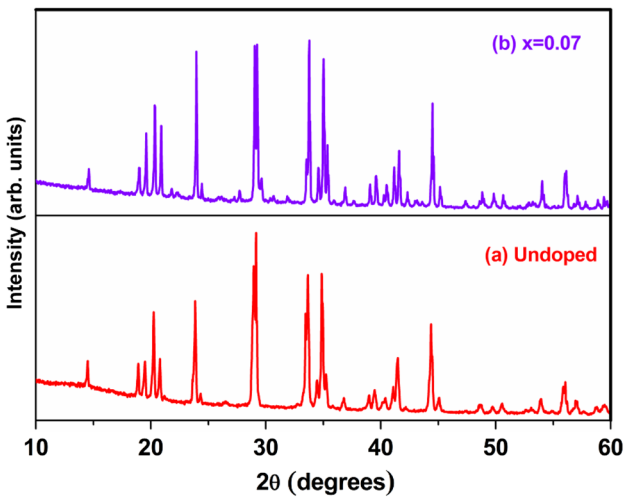

Fig. 1 X-ray diffraction pattern of $LiNa_{3-x}P_2O_7{:}xEu^{3+}$ phosphor: **a** undoped and **b** $x = 0.07$

without other impurity phases. This indicates that the Eu^{3+} ions are incorporated into the $LiNa_3P_2O_7$ host lattice.

3.2 FTIR studies

In order to study the molecular and structural environment of the phosphor, the FTIR spectrum was recorded in the range of 4000–400 cm^{-1}. A typical FTIR spectrum of $LiNa_{3-x}P_2O_7:xEu^{3+}(x = 0.09)$ phosphor is shown in Fig. 2. According to Corbridge et al. [20], FTIR spectrum of the pyrophosphate material shows the evidence of well-known numerous vibrational bands, particularly in four frequency regions, i.e., at v_1 = 3654–3535 cm^{-1} (the O–H stretching of absorbed water), v_2 = 2667–2338 cm^{-1} (C–O vibration of CO_2 in the air), v_3 = 1811–1432 cm^{-1} (the vibration of PO_4^{3-}) and v_4 = 1249–412 cm^{-1} is due to vibration of the P_2O_7 group ($O_3P–O–PO_3$), which can be described for the vibration spectrum interpretation as an assembly of the vibrations of the PO_3 and the P–O–P groups. We note from the spectrum that it consists of two distinct bands around 745 and 924 cm^{-1}, which are assigned to the symmetric and asymmetric vibrational stretching modes of the P–Ô–P bridges. These bands are the characteristic of pyrophosphate groups $(P_2O_7)^{4-}$ (termed as v_4 region) [21]. The strong band centered at 1658 cm^{-1} corresponds to the stretching vibration of PO_4^{3-} groups (termed as v_3 region). Therefore, the obtained results suggest that the prepared material belongs to the diphosphate family.

3.3 Morphology and chemical composition

In order to study the surface morphology of the prepared $LiNa_{3-x}P_2O_7:xEu^{3+}$ phosphor, the SEM measurement was taken. The low- and high-magnified SEM images of $LiNa_{3-x}P_2O_7:xEu^{3+}$ (x = 9 at.%) phosphor are shown in Fig. 3a, b. We note from the figure that the particles possess irregular morphology and are aggregated during the high calcination. A closer look on the high-magnified SEM micrograph certainly indicates the orthorhombic crystal structure of the synthesized phosphor (indicated on Fig. 3b by white circles). From the micrograph, it is clear that various particles have different sizes of the orthorhombic structure and some of them are agglomerated to form the phosphor. However, the average sizes of the particles are in the range of few micrometers. Thus, the defined structure with the micrometer dimension of the phosphor warrants considerable attention in the field of display and lighting. To further examine the purity of the synthesized sample, the EDS spectrum was recorded and is shown in Fig. 4. It revealed the signs of presence of Na, P, O and Eu elements in the prepared samples. However, as expected, Li could not be detected by EDS, since the atomic number is less.

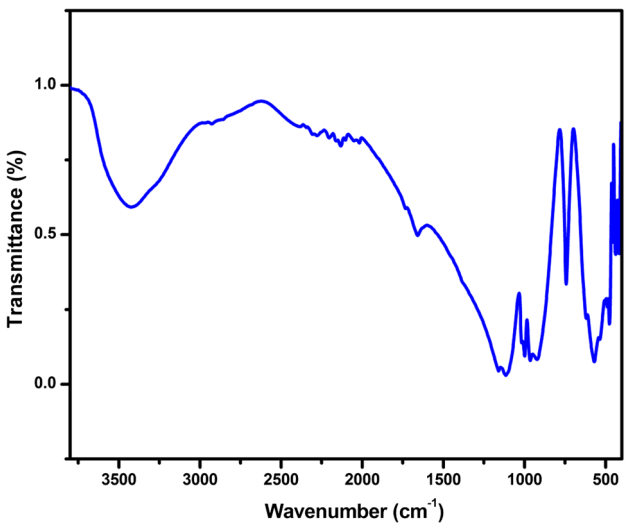

Fig. 2 FTIR spectrum of $LiNa_{3-x}P_2O_7:xEu^{3+}$ (x = 0.09) phosphor

3.4 Diffuse reflectance spectra

To study the energy absorption, UV–Vis DRS of $LiNa_{3-x}P_2O_7:xEu^{3+}$ (x = 5, 7 and 9 at.%) phosphors were recorded and are shown in Fig. 5. As shown in the figure, the absorption peaks appeared at 220–250 nm correspond to charge transfer from O ligands to the central $(PO_4)^{3-}$ groups, while the weak peaks around 400 nm are due to the $4f$–$4f$ inner shell transitions of Eu^{3+} ions [22]. The similar bands were also observed in the excitation spectrum of the phosphor. The bandgap of prepared samples was determined by the Kubelka–Munk (K–M) equation, which converts the reflectance into equivalent absorption spectra [23]. K–M function ($F(R_\alpha)$) is given by:

$$F(R_\alpha) = (1 - R_\alpha)^2 / 2R_\alpha = K/S = \left(hv - E_g\right)^{n/2} / hv \quad (1)$$

where K and S are the absorption and scattering coefficients, respectively, and R_α denotes the diffuse reflectance of an infinitely thick sample. The bandgap E_g and linear absorption coefficient (α) of a material are related through the well-known Tauc relation [24]:

$$[F(R_\alpha)hv]^2 = A\left(hv - E_g\right)^n \quad (2)$$

where A is proportionality constant and hv is the photon energy. Based on the value of n, the transitions can be assigned as follows: n is equal to 1 indicates the existence of direct allowed transitions; 2, non-metallic materials; 3, direct forbidden transitions; 4, indirect allowed transitions; and 6, indirect forbidden transitions [25]. $[F(R\alpha)hv]^2$ versus (hv) graph was plotted and is shown in Fig. 6. The graph was obtained best fitting for $n = 1$, indicating that the

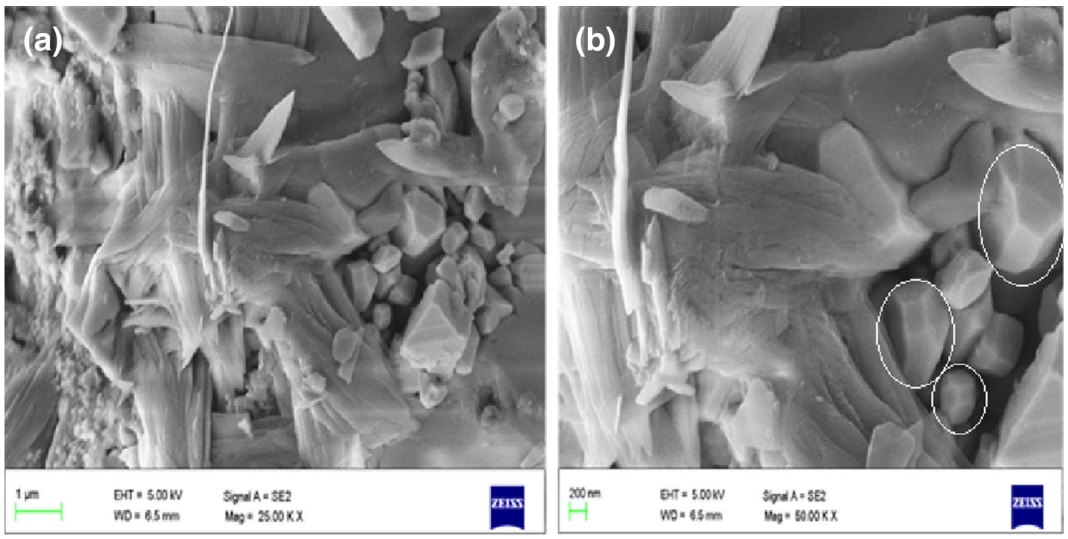

Fig. 3 **a** Low- and **b** high-magnified SEM images of $LiNa_{3-x}P_2O_7{:}xEu^{3+}$ ($x = 0.09$) phosphor

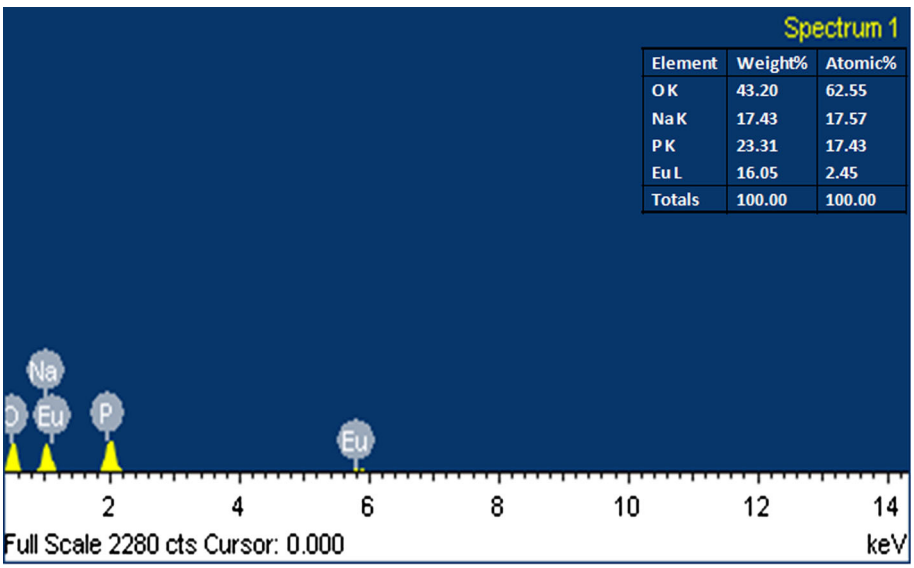

Fig. 4 EDS profile of $LiNa_{3-x}P_2O_7{:}xEu^{3+}$ ($x = 0.09$) phosphor

direct transitions are allowed in the present phosphor. The bandgap energies of phosphors were calculated from graph and found to be varied from 4.75 to 4.9 eV for various concentrations of Eu^{3+} ions.

3.5 Photoluminescence studies

Excitation spectrum of $LiNa_{3-x}P_2O_7{:}xEu^{3+}$ ($x = 9$ at.%) phosphor is shown in Fig. 7. The spectrum showed a weak broad band in the range from 250 to 350 nm, which is assigned to Eu–O charge-transfer band (CTB) transition, and several sharp absorption peaks at around 366, 386, 395 and 420 nm correspond to $^7F_0 \rightarrow {}^5D_4$, $^7F_0 \rightarrow {}^5L_7$, $^7F_0 \rightarrow {}^5L_6$ and $^7F_0 \rightarrow {}^5D_3$ transitions of Eu^{3+} ions, respectively [26, 27]. Among the sharp lines, the absorption band at 395 nm is strongest, which is assigned to $^7F_0 \rightarrow {}^5L_6$ transition of Eu^{3+} ions and is used to measure the emission spectra of the phosphors. Therefore, it clearly indicates that the prepared phosphor could strongly absorb the ultraviolet light, which is matched well with the characteristic emission of the near-UV LED chips [28].

To further investigate the effect of Eu^{3+} concentration on $LiNa_{3-x}P_2O_7{:}xEu^{3+}$ ($x = 1$–9 at.%) phosphors, the photoluminescence emission spectra were recorded. Figure 8 shows the emission spectra of phosphors under 395-nm excitation. The emission band covers a region from 580 to 630 nm and includes several distinct emission bands. These bands were ascribed to the transition from $^5D_0 \rightarrow {}^7F_J$ ($J = 0, 1, 2$) of Eu^{3+} ions [29]. From the emission spectra, it was observed that the orange emission

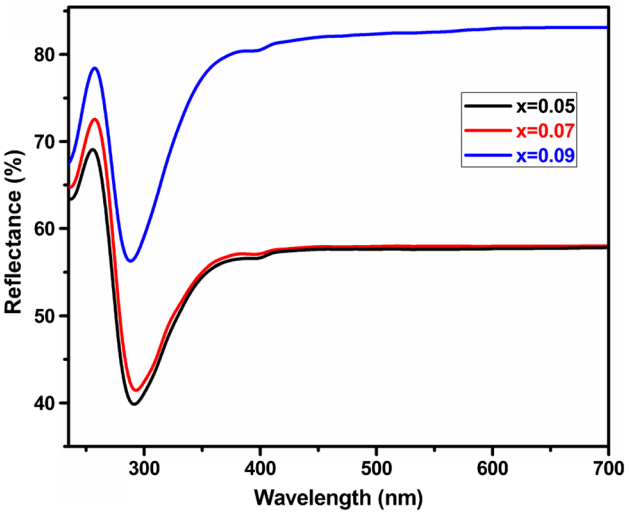

Fig. 5 Diffuse reflectance spectra of $LiNa_{3-x}P_2O_7:xEu^{3+}$ ($x = 0.05$–0.09) phosphor

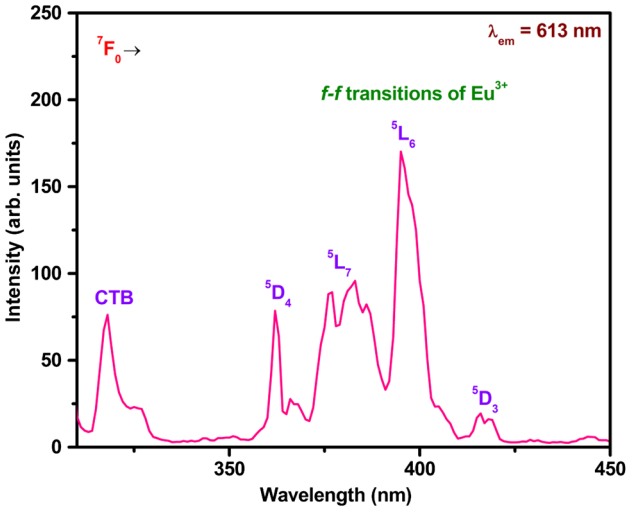

Fig. 7 Excitation spectrum of $LiNa_{3-x}P_2O_7:xEu^{3+}$ ($x = 0.09$) phosphor

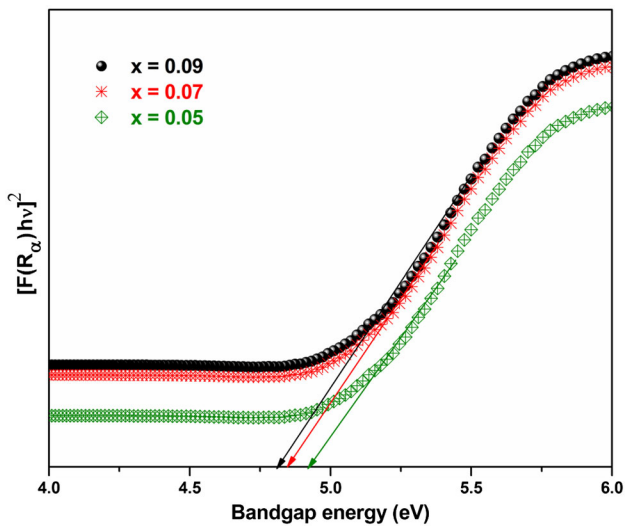

Fig. 6 K–M function versus photon energy of $LiNa_{3-x}P_2O_7:xEu^{3+}$ ($x = 0.05$–0.09) phosphor

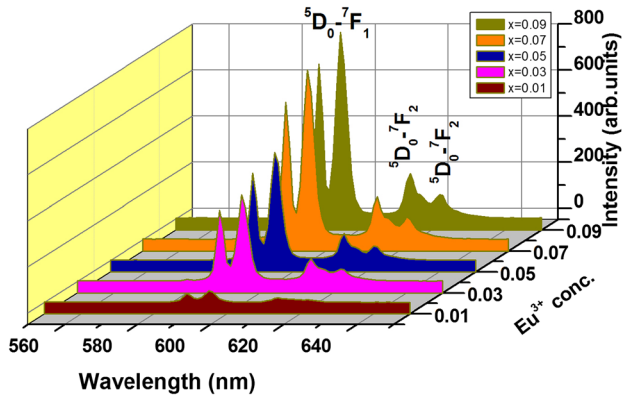

Fig. 8 PL emission spectra of $LiNa_{3-x}P_2O_7:xEu^{3+}$ ($x = 0.01$–0.09) phosphor at 395-nm excitation

peaks at 585 and 595 nm due to the magnetic dipole (MD) transition ($^5D_0 \rightarrow {}^7F_1$) are dominant than a very weak shoulder around 581 nm that corresponds to the $^5D_0 \rightarrow {}^7F_0$ transition. The emission bands at 615 and 623 nm (in red region) were attributed to the $^5D_0 \rightarrow {}^7F_2$ electric dipole (ED) transitions [30]. The emission due to $^5D_0 \rightarrow {}^7F_2$ ED transition is hypersensitive to the symmetry of crystal field environment, while the $^5D_0 \rightarrow {}^7F_1$ MD transition is insensitive to the site symmetry and hardly varies with the environment, because it is parity-allowed [31]. It is noteworthy that if the Eu^{3+} ions occupy the inversion symmetry center, the MD transition ($^5D_0 \rightarrow {}^7F_1$) dominates the ED transition $^5D_0 \rightarrow {}^7F_2$. In the present case, the $^5D_0 \rightarrow {}^7F_1$ transition is dominant, indicating that the Eu^{3+} ions are located at high symmetry positions.

The luminescence intensity ratio (R) values,

$$I_e(^5D_0 \rightarrow {}^7F_2)/I_m(^5D_0 \rightarrow {}^7F_1), \quad (3)$$

Widely known as asymmetric ratio, allow the estimation of the covalent nature, polarization of the surrounding of the Eu^{3+} ions by short-range effects and centro-symmetry distortion of Eu^{3+} ion site. The lower the value of R, the higher the symmetry around the Eu^{3+} ions and the higher the Eu–O covalence and vice versa [32]. The R values of $LiNa_{3-x}P_2O_7:xEu^{3+}$ phosphors were calculated and found to be 0.42, 0.31, 0.25, 0.24 and 0.23 for $x = 0.01$, 0.03, 0.05, 0.07 and 0.09, respectively. The decrease in asymmetric ratio revealed a relatively high local symmetry around the Eu^{3+} in $LiNa_3P_2O_7$. Further, it could be concluded that the prepared phosphors will convert near-UV radiation to more orange emission due to MD transitions

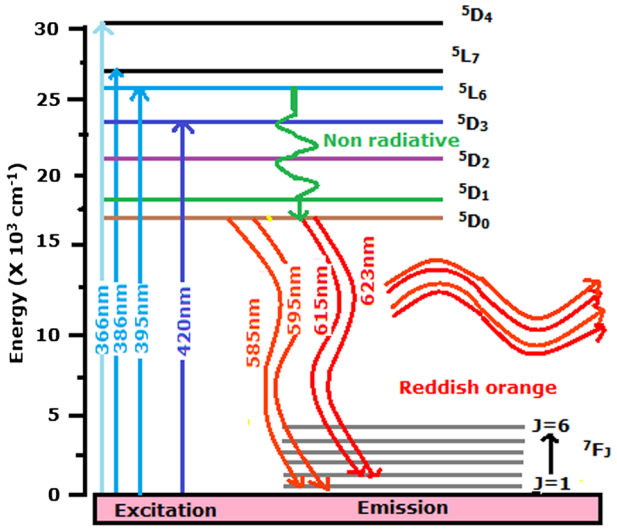

Fig. 9 Schematic energy-level diagram of Eu^{3+} ions in $LiNa_3P_2O_7$ host

than red emission due to ED transitions. The transitions of Eu^{3+} ions in host $LiNa_3P_2\_O_7\_$ phosphor are represented by the energy-level diagram which is shown in Fig. 9. Further, in order to find the effect of Eu^{3+} dopant concentration on $LiNa_{3-x}P_2O_7$:xEu^{3+} phosphor, the percentage of Eu was varied in the host from $x = 1$–9 at.%. Unfortunately, we could not find any quenching up to 9 at.%, and this may be due to more bandgap energy of host matrix, which was calculated from K–M function.

3.6 Judd–Ofelt parameters

The Judd–Ofelt (J–O) theory is considered very vital for analyzing the spectral properties of lanthanide ions (Ln^{3+}) in the hosts and is extensively used for describing 4*f* optical transition intensities of trivalent rare-earth ions in various hosts [30]. In order to study the site symmetry and luminescence behavior of Eu^{3+} ions in the host and also to predict some important radiative properties such as radioactive transition probability (A), branching ratios (β_R), stimulated emission cross section (σ) and radioactive lifetime (τ_R) transition probabilities, J–O parameters (Ω_2, Ω_4 and Ω_6) have been evaluated. The polarization and electric dipole transition of the Eu^{3+} ions could be determined by intensity parameter (Ω_2), whereas the other two intensity parameters $\Omega_{4,6}$ depend on long-range effects. In general, these intensity parameters are used to understand the radiative potential properties of RE ions in different host matrices. In the present work, these parameters are calculated from the luminescence emission spectra of the phosphors, because of the difficulty in analyzing the absorption spectrum of powder phosphors [25, 33]. The intensity parameters are connected to coefficients of spontaneous emission (A_{0J}) through the relation:

$$A_{OJ} = \frac{64\pi^4\vartheta^3}{3hc^3}\frac{e^2n(n^2+2)^2}{9(4\pi\varepsilon_o)}\sum_{\lambda=2,4,6}\Omega_\lambda\left\langle \Psi' J' \parallel U^\lambda \parallel \psi J\right\rangle^2 \tag{4}$$

where ϑ is the frequency, h is the Planck constant, e is the charge of the electron, $1/4\pi\varepsilon_0$ is the constant, $\frac{n(n^2+2)^2}{9}$ is the Lorentz field correction, and n is the refractive index of the material. The term $\left\langle \Psi' J' \parallel U^\lambda \parallel \psi J\right\rangle^2$ is square of the reduced matrix elements. The reduced matrix elements of Eu^{3+} ions for $^5D_0 \rightarrow {}^7F_2$ transition ($U^2 = 0.0032$) and $^5D_0 \rightarrow {}^7F_4$ ($U^4 = 0.0023$) were taken from the reported values by Carnell et al. [34]. The experimental coefficients of spontaneous emission (A_{0J}) could be estimated according to the relation:

$$A_{0J} = A_{01}\left(\frac{I_{OJ}}{I_{01}}\right)\left(\frac{\vartheta_{01}}{\vartheta_{OJ}}\right) \tag{5}$$

where υ_{01} and υ_{0J} ($J = 2, 4$) represent the frequency of the transitions $^5D_0 \rightarrow {}^7F_1$ and $^5D_0 \rightarrow {}^7F_{J\,=\,2,4}$ for Eu^{3+}, respectively, and A_{01} is known as Einstein's coefficient of spontaneous emission corresponding to magnetic dipole transition for either ions. For Eu^{3+}, A_{01} can be determined to be 50 s^{-1} and I_{0J} is the integrated intensity of the transition $\left\langle \Psi' J' \parallel U^\lambda \parallel \psi J\right\rangle^2$ [35]. Generally, refractive index is necessary in calculating the intensity parameters Ω_λ ($\lambda = 2$, 4, 6) using Judd–Ofelt theory. However, refractive index is sometimes quite difficult to measure in case of crystalline powder sample. To our knowledge, the refractive index value of $LiNa_3P_2O_7$ host matrix is not reported in the literature. However, by considering the quite similar crystal structure between $LiNa_3P_2O_7$and $Li_2BaP_2O_7$, and compared to the calculated results of different phosphate crystals, the refractive index value generally ranges from 1.4 to 1.8 [36]. Therefore, in the present investigation, the authors considered the refractive index value of 1.8 for the prepared phosphor to calculate the J–O parameters.

The experimental intensity parameter Ω_λ ($\lambda = 2$) was determined using the emission spectra of Eu^{3+}-doped $LiNa_3P_2O_7$ phosphors. Usually, Eu^{3+} exhibits various emission bands ranging from 580 to 650 nm. Among them, the $^5D_0 \rightarrow {}^7F_1$ transition is allowed magnetic dipole transition that is independent of local environment, while the other $^5D_0 \rightarrow {}^7F_2$ transition is permitted as electric dipole transition at low symmetries with no inversion centers [34]. From Eqs. 4 and 5, the value of Ω_2 for $LiNa_{3-x}P_2O_7$:xEu^{3+}($x = 0.01$–0.09) was calculated and is presented in Table 1. Moreover, the values of Ω_4 and Ω_6 could not be

Table 1 Calculated optical parameters of $LiNa_3P_2O_7:Eu^{3+}$ phosphor

Concentration (at.%)	Transitions	A_T (s^{-1})	A_{0-2} (s^{-1})	Ω_2 (pm^2)	τ_{rad} (ms)	β (%)	σ (λp) (10^{-22} cm^2)	Gain bandwidth (10^{-28} cm^2)
1	$^5D_0$–$^7F_1$	1.20	0.98	–	83	81	0.31	0.14
	$^5D_0$–$^7F_2$	–	0.22	0.168		18	0.09	0.03
3	$^5D_0$–$^7F_1$	12.84	10.60	–	77	82	0.64	0.29
	$^5D_0$–$^7F_2$	–	2.24	0.199		17	0.24	0.12
5	$^5D_0$–$^7F_1$	14.15	11.17	–	70	78	0.83	0.42
	$^5D_0$–$^7F_2$	–	2.98	0.252		21	0.28	0.14
7	$^5D_0$–$^7F_1$	15.75	12.15	–	63	77	0.92	0.55
	$^5D_0$–$^7F_2$	–	3.6	0.272		22	0.32	0.19
9	$^5D_0$–$^7F_1$	15.95	12.25	–	62	76	1.08	0.63
	$^5D_0$–$^7F_2$	–	3.70	0.284		23	0.37	0.22

estimated, since the emission spectrum of Eu^{3+} consists of only the $^5D_0 \rightarrow {}^7F_2$ transition.

3.7 Radiative properties

The radioactive transition probability (A_T) for a transition from an excited manifold J to a lower manifold J_0 can be calculated by $\Psi J - \Psi' J'$, which is obtained by the sum of electric (A_{ed}) and magnetic (A_{md}) dipole radiative transition probabilities [34]:

$$A_T(\Psi J\,,\,\Psi' J') = A_{ed} + A_{md}, \tag{6}$$

The electric (A_{ed}) and magnetic (A_{md}) dipole radiative transition probabilities are evaluated by the following expressions:

$$A_{ed} = \frac{64\pi^4\vartheta^3}{3h(2J+1)}\frac{e^2 n(n^2+2)^2}{9} \times s_{ed} \quad \text{and}$$
$$A_{md} = \frac{64\pi^4\vartheta^3}{3h(2J+1)}(n)^3 \times s_{md} \tag{7}$$

where S_{ed} is electric dipole line strength $e^2\sum_{i=2,4,6}\Omega_i\left(\Psi J \parallel U^{\lambda} \parallel \Psi' J'\right)^2$ and S_{md} is magnetic dipole line strength $\frac{e^2h^2}{16\pi^2m^2c^2}\left(\Psi J \parallel L+2s \parallel \Psi' J'\right)^2$. The total radiative transition probability (A_T) for an excited state is given as the sum of the $A(\Psi J,\ \Psi' J')$ terms calculated over all the terminal states $A_T(\Psi J,\ \Psi' J') = \sum_{\Psi' J'} A(\Psi J, \Psi' J')$. The fluorescence branching ratio (β_R) of each of the transitions is determined from the spontaneous transition probability according to the equation:

$$\beta_R(\Psi J, \Psi' J') = \frac{A(\Psi J, \Psi' J')}{A_T(\Psi J, \Psi' J')} \tag{8}$$

The rate of depopulation of an excited state is given by the radiative lifetime (τ_R)

$$\tau_R(\Psi J, \Psi' J') = \frac{1}{A_T(\Psi J, \Psi' J')} \tag{9}$$

In order to identify the potential laser transitions of Eu^{3+} ions in host material, the stimulated emission cross section ($\sigma_{(\lambda p)}$) has been used. From literature reviews, a good laser transition can have large stimulated emission cross section and is the attractive feature for low-threshold, high-gain laser applications, which are used to obtain continuous-wave laser action. The peak stimulated emission cross section is as given below

$$\sigma_{(\lambda p)}(\Psi J,\ \Psi' J') = \frac{\lambda_p^4}{8\pi c n^2 \Delta\lambda_{\text{eff}}} A(\Psi J, \Psi' J') \tag{10}$$

The gain bandwidth ($\sigma_{(\lambda p)} \times \Delta\lambda p$) is one of the parameters that are critical to predict the amplification of the medium in which the RE ions are situated. A good optical amplifier should have larger $\sigma_{(\lambda p)}$ and ($\sigma_{(\lambda p)} \times \Delta\lambda p$) values. The Judd–Ofelt intensity parameters and the spectral parameters are presented in Table 1.

3.8 Chromaticity coordinates

The CIE (International Commission on Illumination) chromaticity coordinates (x, y) and CCT (correlated color temperature) values of $LiNa_3P_2O_7$ phosphors were calculated to characterize the color emission from their corresponding emission spectra. The obtained color coordinates of these samples lie in the red region as shown in Fig. 10. We note from the figure that the color coordinates traversed a wide range from the red region to orange region, and the changes in the color coordinates may be due to the variation of the asymmetric ratios of various concentrations of Eu^{3+} ion in $LiNa_3P_2O_7$ phosphors. The CCT values are calculated by using the McCamy's [37] empirical formula which is given by

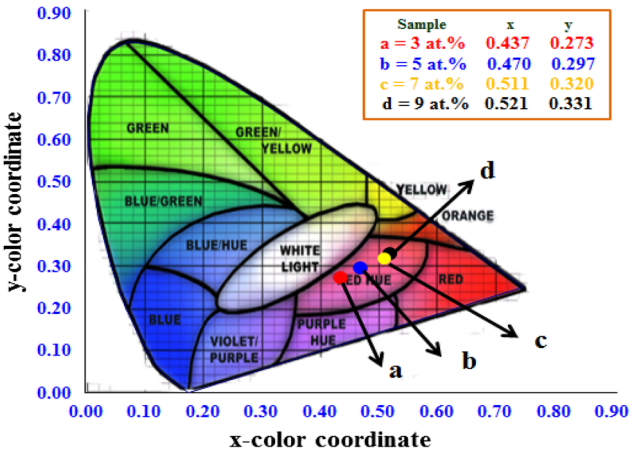

Fig. 10 CIE chromaticity diagram of $LiNa_{3-x}P_2O_7{:}xEu^{3+}$ ($x = 0.03$–0.09)

Table 2 CIE coordinates and CCT values of Eu^{3+}-doped $LiNa_3P_2O_7$ phosphor

Dopant concentration (at.%)	Color coordinates		CCT (K)
	x	y	
3	0.437	0.273	1630
5	0.470	0.297	1624
7	0.511	0.320	1622
9	0.521	0.331	1619

$$CCT = -449n^3 + 3525n^2 - 6823.3n + 5520.33 \quad (11)$$

where $n = (x - x_e)/(y - y_e)$ and chromaticity epicenter is at $x_e = 0.3320$ and $y_e = 0.1858$. The estimated color coordinates and CCT values are presented in Table 2. The CCT values of the studied phosphors were found to be 1620 K.

4 Conclusion

A new series of $LiNa_{3-x}P_2O_7{:}xEu^{3+}$ ($x = 0.01$ to 0.09) phosphors were synthesized by the solid-state method. The phosphors were crystallized in the orthorhombic structure. The pyrophosphate groups in the phosphors were confirmed by FTIR. Interestingly, the orthorhombic structural morphology of the synthesized phosphor in the micrometer dimension was identified by SEM images. Under 395-nm light irradiation, the Eu^{3+}-doped $LiNa_3P_2O_7$ phosphors show red emission around 613 nm. Furthermore, The J–O parameter (Ω_2) and luminescence intensity ratio (R) were calculated from the emission spectra. The color coordinates were located in the red region. Therefore, the obtained results suggest that the proposed phosphor may have potential application as a red emitter in the display and lighting devices.

Acknowledgments One of the authors, B. Deva Prasad Raju, is highly grateful to DST-SERB, Department of Science and Technology, Government of India, India, for providing financial assistance in the form of Fast Track Research Project (Young Scientist Award); vide reference number: DST-SR/FTP/PS-198/2012; dated-14-02-2014.

References

1. M. Zeuner, P.J. Schmidt, W. Schnick, Chem. Mater. **21**, 2467 (2009)
2. C. Liu, Z. Xia, Z. Lian, J. Zhou, Q. Yan, J. Mater. Chem. C **1**, 7139 (2013)
3. M. Zhang, J. Wang, W. Ding, Q. Zhang, Q. Su, Appl. Phys. B **86**, 647 (2007)
4. Y. Li, H. Li, B. Liu, J. Zhang, Z. Zhao, Z. Yang, Y. Wen, Y. Wang, J. Phys. Chem. Solids **74**, 175 (2013)
5. P. Li, Z. Wang, Z. Yang, Q. Guo, X. Li, J. Lumin. **130**, 222 (2010)
6. J. Sun, X. Zhang, Z. Xia, H. Du, J. Appl. Phys. **111**, 013101 (2012)
7. G.R. Dillip, K. Mallikarjuna, S.J. Dhoble, B. Deva, Prasad. J. Phys. Chem. Solids **75**, 8 (2014)
8. S.P. Lee, T.S. Chan, T.M. Chen, A.C.S. Appl, Mater. Interfaces **7**, 40 (2015)
9. J.K. Han, A. Piqutte, M.E. Hannah, G.A. Hirata, J.B. Talbot, K.C. Mishra, J. Lumin. **148**, 1 (2014)
10. T.G. Kim, H.S. Lee, C.C. Lin, T. Kim, R.S. Liu, T.S. Chan, S.J. Im, Appl. Phys. Lett. **96**, 061904 (2010)
11. R.J. Wiglusz, T. Grzyb, A. Lukowiak, A. Bednarkiewicz, S. Lis, W. Strek, J. Lumin. **133**, 102 (2012)
12. V.B. Pawade, S.J. Dhoble, J. Lumin. **135**, 318 (2013)
13. F. Yang, Y. Liang, M. Liu, X. Li, M. Zhang, N. Wang, Opt. Laser Technol. **46**, 14 (2013)
14. G. Li, Q. Cao, Z. Li, Y. Huang, J. Rare Earths **26**, 792 (2008)
15. A. Hakeem, K.N. Shinde, S.J. Yoon, S.J. Dhoble, K. Park, J. Nanosci. Nanotechnol. **14**, 5873 (2014)
16. J. Lü, Y. Huang, L. Shi, H.J. Seo, Appl. Phys. A **99**, 859 (2010)
17. S. Chen, Y. Wang, J. Zhang, L. Zhao, Q. Wang, L. Han, J. Lumin. **150**, 46 (2014)
18. Y. Shi, Y. Wang, S. Pan, Z. Yang, X. Dong, H. Wu, J. Solid State Chem. **197**, 128 (2013)
19. A. Zaafouri, M. Megdiche, M. Gargouri, J. Alloys Compd. **584**, 152 (2014)
20. D.E. Corbridge, in *Topics in Phosphorus Chemistry*, ed. by M. Grayson, E.J. Griffith (New York, 1966), p. 275
21. R.L. Kohale, S.J. Dhoble, J. Alloys Compd. **586**, 314 (2014)
22. G.R. Dillip, B.D.P. Raju, J. Alloys Compd. **540**, 67 (2012)
23. P. Kubelka, F.Z. Munk, Z. Tech, Phys. (Leipzig) **12**, 593 (1931)
24. J. Tauc, A. Menth, J. Non Cryst. Sol. **8**, 569 (1972)
25. S. Som, A.K. Kunti, V. Kumar, V. Kumar, S. Dutta, M. Chowdhury, S.K. Sharma, J.J. Terblans, H.C. Swart, J. Appl. Phys. **115**, 193101 (2014)
26. P. Yu, L. Su, J. Xu, Opt. Rev. **21**, 455 (2014)
27. S. Zhang, Y. Nakai, T. Tsuboi, Y. Huang, H.J. Seo, Chem. Mater. **23**, 1216 (2011)
28. B. Han, J. Zhang, Z. Wang, Y. Liu, H. Shi, J. Lumin. **149**, 150 (2014)
29. R. Wang, L. Zhou, Y. Wang, J. Rare Earths **29**, 1045 (2011)
30. G.R. Dillip, S.J. Dhoble, L. Manoj, C.M. Reddy, B.D.P. Raju, J. Lumin. **132**, 3072 (2012)
31. E. Song, W. Zhao, G. Zhou, X. Dou, C. Yi, M. Zhou, J. Rare Earths **29**, 440 (2011)

32. A.K. Parchur, A.I. Prasad, S.B. Rai, R. Tewari, R.K. Sahu, G.S. Okram, R.A. Singh, R.S. Ningthoujam, AIP Adv. **2**, 032119 (2012)
33. H. Xia, J. Feng, Y. Ji, J. Xu, Z. Zhu, Y. Wang, Z. You, J. Li, H. Wang, C. Tu, J. Lumin. **149**, 7 (2014)
34. W.T. Carnall, P.R. Fields, K. Rajnak, J. Chem. Phys. **49**, 4253 (1968)
35. M. Ferhi, C. Bouzidi, K. Horchani-Naifer, H. Elhouichet, M. Ferid, J. Lumin. **157**, 21 (2015)
36. V. Kumar, S. Som, V. Kumar, V. Kumar, O.M. Ntwaeaborwa, E. Coetsee, H.C. Swart, Chem. Eng. J. **255**, 541 (2014)
37. C.S. McCamy, Color. Res. Appl. **17**, 142 (1992)